Figures and figure supplements

Spontaneous neural synchrony links intrinsic spinal sensory and motor networks during unconsciousness

Jacob Graves McPherson and Maria F Bandres

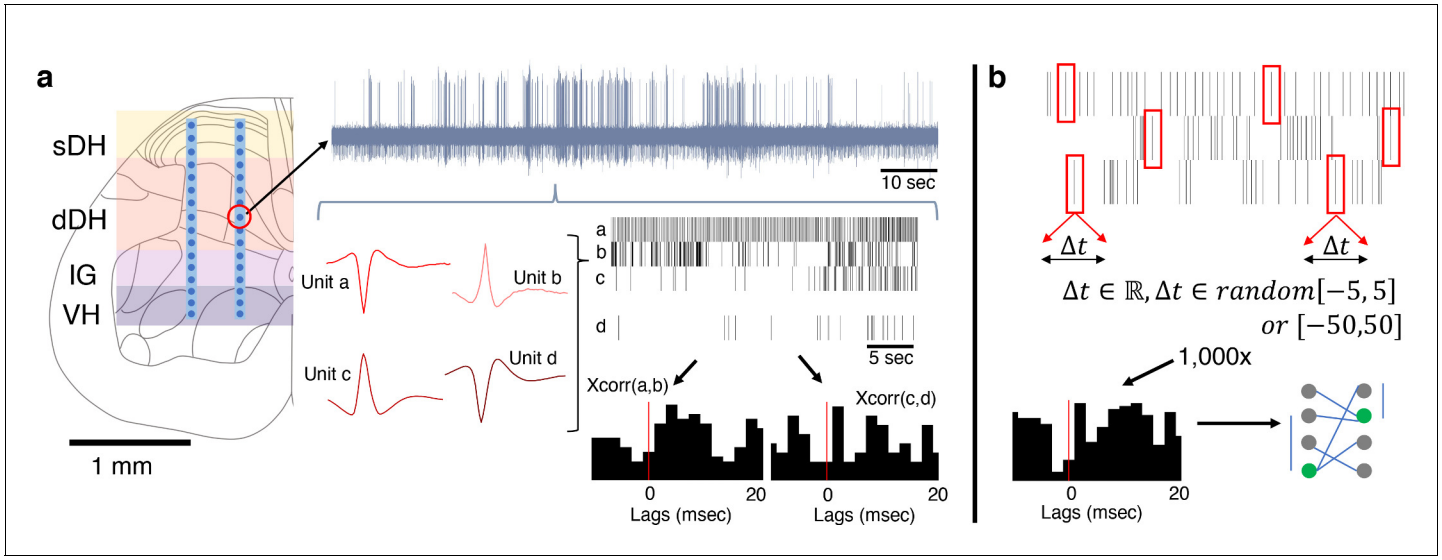

Figure 1. Experimental setup and design. (**a**) Dual-shank microelectrode arrays with 32 independent recording contacts were implanted into the spinal cord at the L5 dorsal root entry zone. Electrodes spanned the superficial dorsal horn (sDH), deep dorsal horn (dDH), intermediate gray matter (IG), and the ventral horn (VH). Multi-unit neural activity was recorded from each electrode (e.g., upper gray trace) and discriminated offline into spike trains of individual units (red single-unit waveforms and spike train raster plots depict four units found on a single channel). Temporal synchrony between spontaneously co-active units was then analyzed via correlation-based approaches (cross-correlation 'xcorr' histograms below rasters, vertical red lines illustrate the 0 ms lag point). (**b**) Illustration of procedure for generating the synthetic dataset. Each spike, from every identified neuron in every trial, was randomly jittered by [−5:5] ms or, separately, [−50:50] ms. The jittered data were then reconstructed, forming synthetic trials containing neurons with firing properties that were statistically similar to the observed data. This process was then repeated over 1000× to generate a large synthetic dataset from which to sample. Spatiotemporal correlation analyses then proceeded on this synthetic dataset to benchmark the empirically observed data.

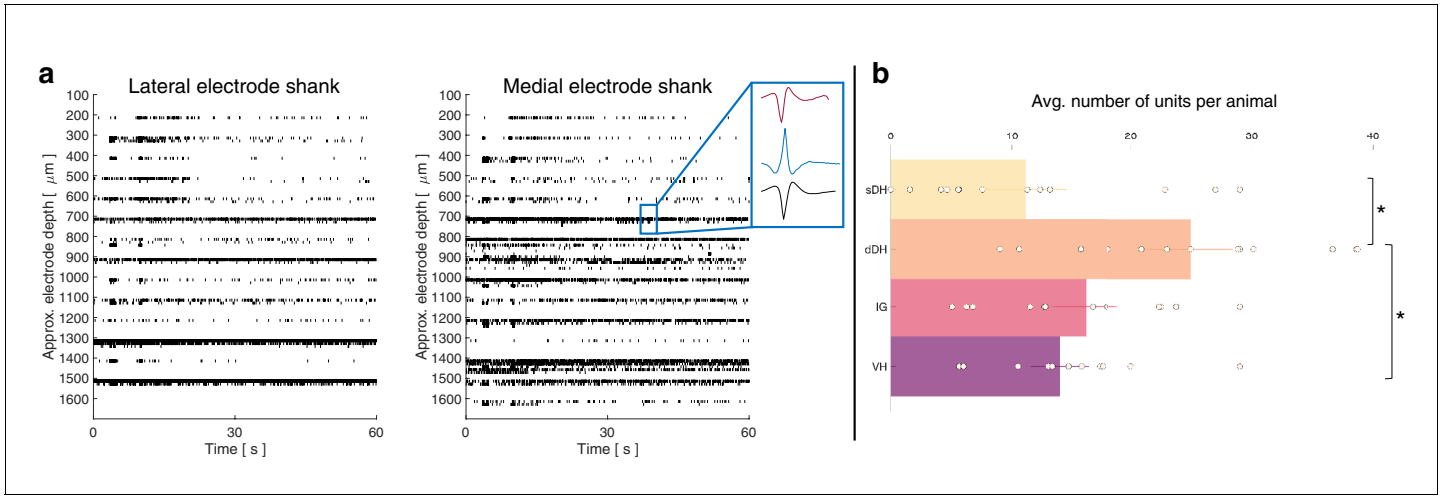

Figure 2. Spontaneous neural transmission is broadly evident across all spatial and functional regions of the spinal gray matter. (**a**) Raster plot of spontaneously active neurons. Each row of hatches represents a discrete neuron. Inset depicts representative spike waveforms discriminated from a single electrode. X-axes (time) are synchronized across the two subplots. (**b**) Distribution of spontaneously active units per gross anatomical region across animals in the urethane cohort (μ ± sem; *N* = 13 animals). The deep dorsal horn contained significantly more spontaneously active units on average than the superficial dorsal horn or ventral horn, driving an overall main effect of region (p=0.001).

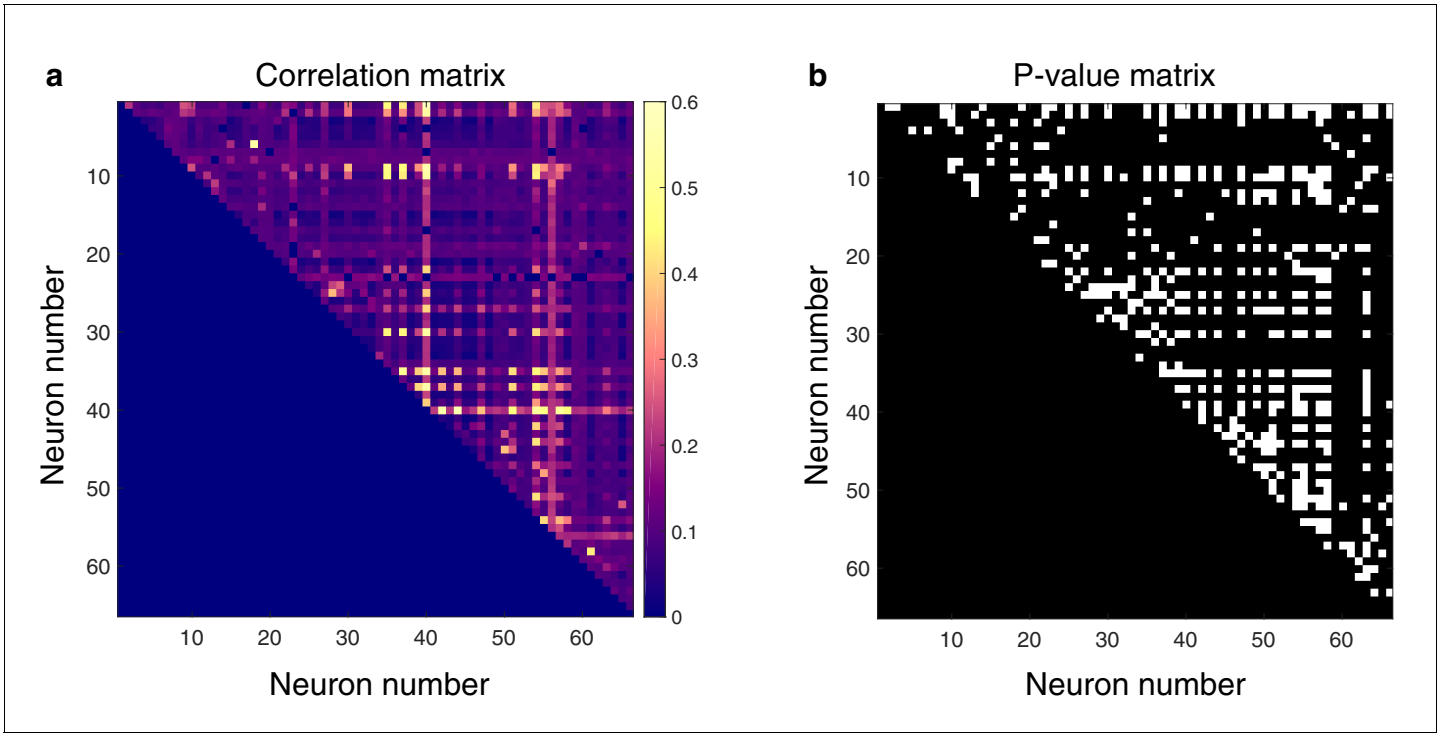

Figure 3. Spontaneously active units exhibit temporal synchrony. For both plots, rows and columns are ordered from 1 *N*, where *N* is the total number of units discriminated for a given trial. (**a**) Strength of temporal correlation between pairs co-active units, indicated by pixel color. Pixels below identity line are omitted because reciprocal connections were not considered. (**b**) Statistical matrix of correlation strength show in panel (**a**). White pixels represent statistically significant correlations, here defined as those with p-values ≤ 0.02. Of the 66 total spontaneously active units discriminated in this epoch, and thus 2145 possible unique connections (ignoring reciprocal connections), 438 pairs exhibited significantly correlated temporal discharge.

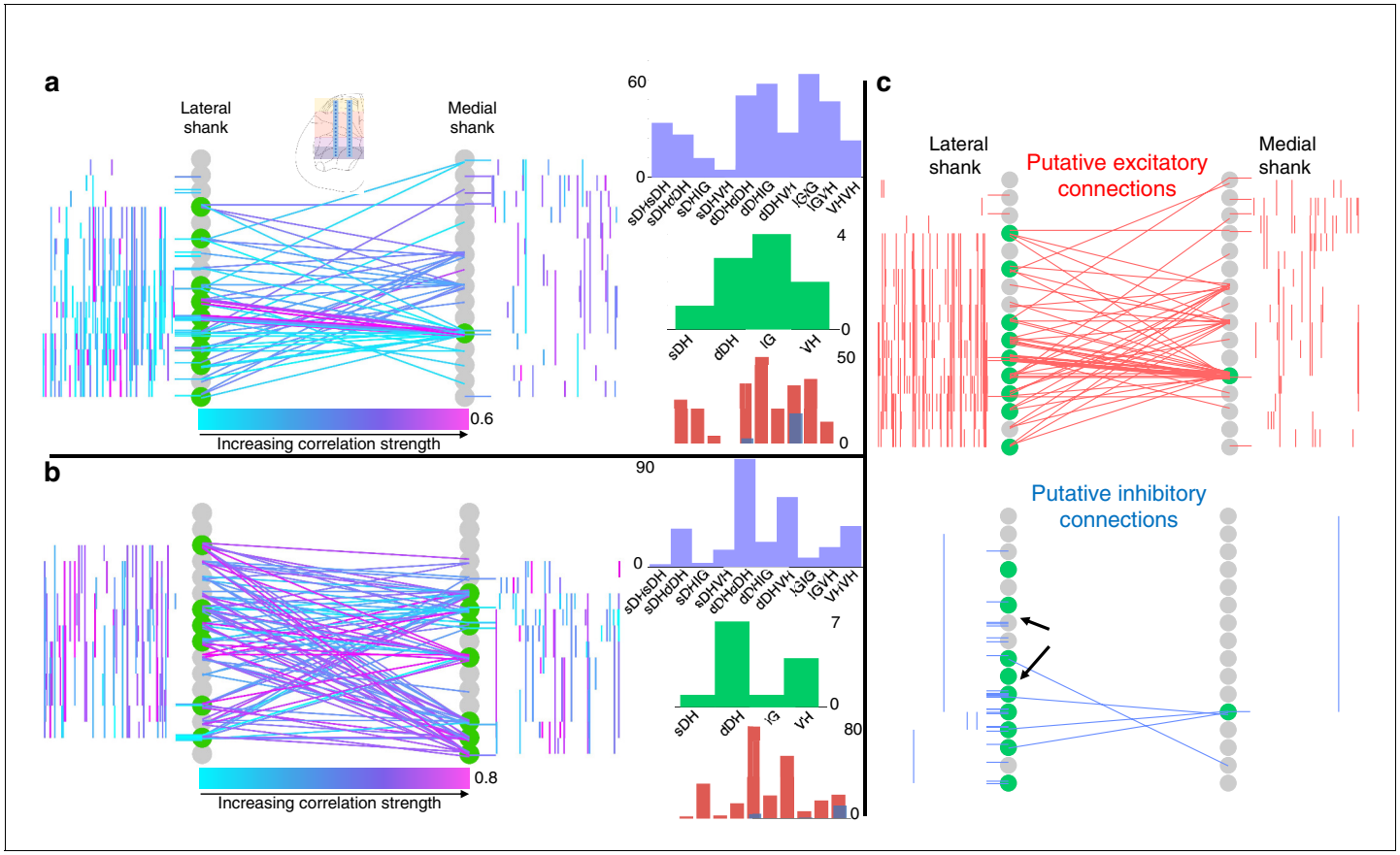

Figure 4. Topology of spontaneously synchronous unit pairs is not relegated to regions of primary afferent terminations, rather it links sensory- and motor-dominant regions of the spinal cord. Representative functional connectivity maps from two animals (panels **a** and **b** from same animal; panel **c** from separate animal). For all topology plots (**a–c**): spinal cord inset image in panel (**a**) shows electrode location. Gray circles represent individual electrodes on the microelectrode array. Green highlighted circles were determined to be the most connected nodes of the recording. Colored lines represent significantly correlated temporal discharge between pairs of spontaneously active units at the indicated locations (note: horizontal lines indicate connections between units discriminated from a single electrode, vertical lines are connections between units on the same shank). For panels (**a**) and (**b**), line color delineates increasing correlation strength from blue to violet; for panel (**c**), red lines indicate putative excitatory connections, blue lines indicate putative inhibitory connections. In panels (**a**) and (**b**), histograms depict the following (top to bottom): purple histograms indicate the overall anatomical distribution of significant connections (in order left to right: sDH-sDH, sDH-dDH, sDH-IG, sDH-VH, dDH-dDH, dDH-IG, dDH-VH, IG-IG, IG-VH, VH-VH); green histograms indicate the gross anatomical distribution of most connected nodes (in order left to right: sDH, dDH, IG, VH); and red/blue histograms indicate the distribution of putative excitatory and inhibitory connections, respectively, in same order as purple histograms above. Black arrows in panel (**c**), inhibitory connections, are intended simply to highlight the preponderance of within-electrode connections. sDH: superficial dorsal horn; dDH: deep dorsal horn; IG: intermediate gray matter; VH: ventral horn.

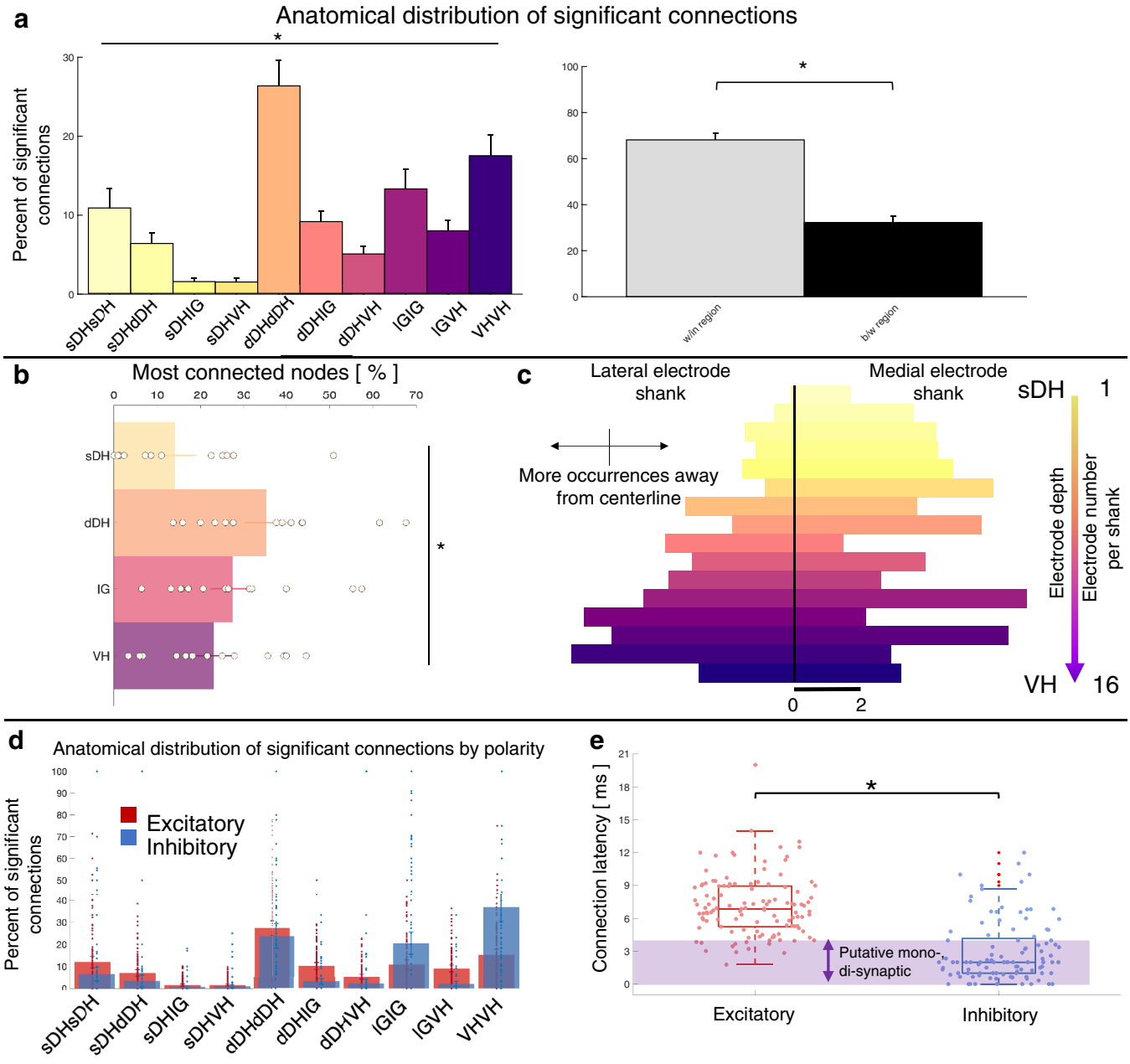

Figure 5. Summary of topological data for urethane-anesthetized animals. (**a**) Proportion of significant connections by anatomical region (*N* = 13 animals). From left to right, bar plots indicate connections from sDH-sDH, sDH-dDH, sDH-IG, sDH-VH, dDH-dDH, dDH-IG, dDH-VH, IG-IG, IG-VH, and VH-VH. Darkening color gradient from left to right qualitatively indicates depth from dorsal surface of spinal cord. Grayscale plots are the proportion of within- and between-region connections, respectively. Significant connections are not uniformly distributed anatomically, with an overall main effect of connection location ($p<0.0001$) and significantly more within-region than between-region connections ($p<0.0001$). (**b**) Gross anatomical distribution of the most connected nodes (*N* = 13 animals). From top to bottom (light to dark): sDH, dDH, IG, and VH. Significant main effect of anatomical region on proportion of most connected nodes, $p=0.009$. (**c**) Histogram of most connected nodes across electrodes on each shank. Bars to left of vertical black line reflect lateral electrode shank, and bars to right of vertical black line reflect medial electrode shank; from top to bottom (light to dark), each row represents one electrode (16 total rows). Bar length indicates the number of occurrences that electrode was determined to be in the 'most connected' subset. (**d**) Spatial distribution: proportion of significant connections by polarity (excitatory, inhibitory) and anatomical region. Red bars: putative excitatory connections; blue bars: putative inhibitory connections. (**e**) Temporal distribution: latencies of significant excitatory (red) and inhibitory (blue) connections. Purple shaded region intended to highlight latencies compatible with potential monosynaptic or disynaptic connections. Inhibitory

Figure 5 continued on next page

Figure 5 continued

latencies were significantly shorter than excitatory latencies on average (p=0.0003). sDH: superficial dorsal horn; dDH: deep dorsal horn; IG: intermediate gray matter; VH: ventral horn.

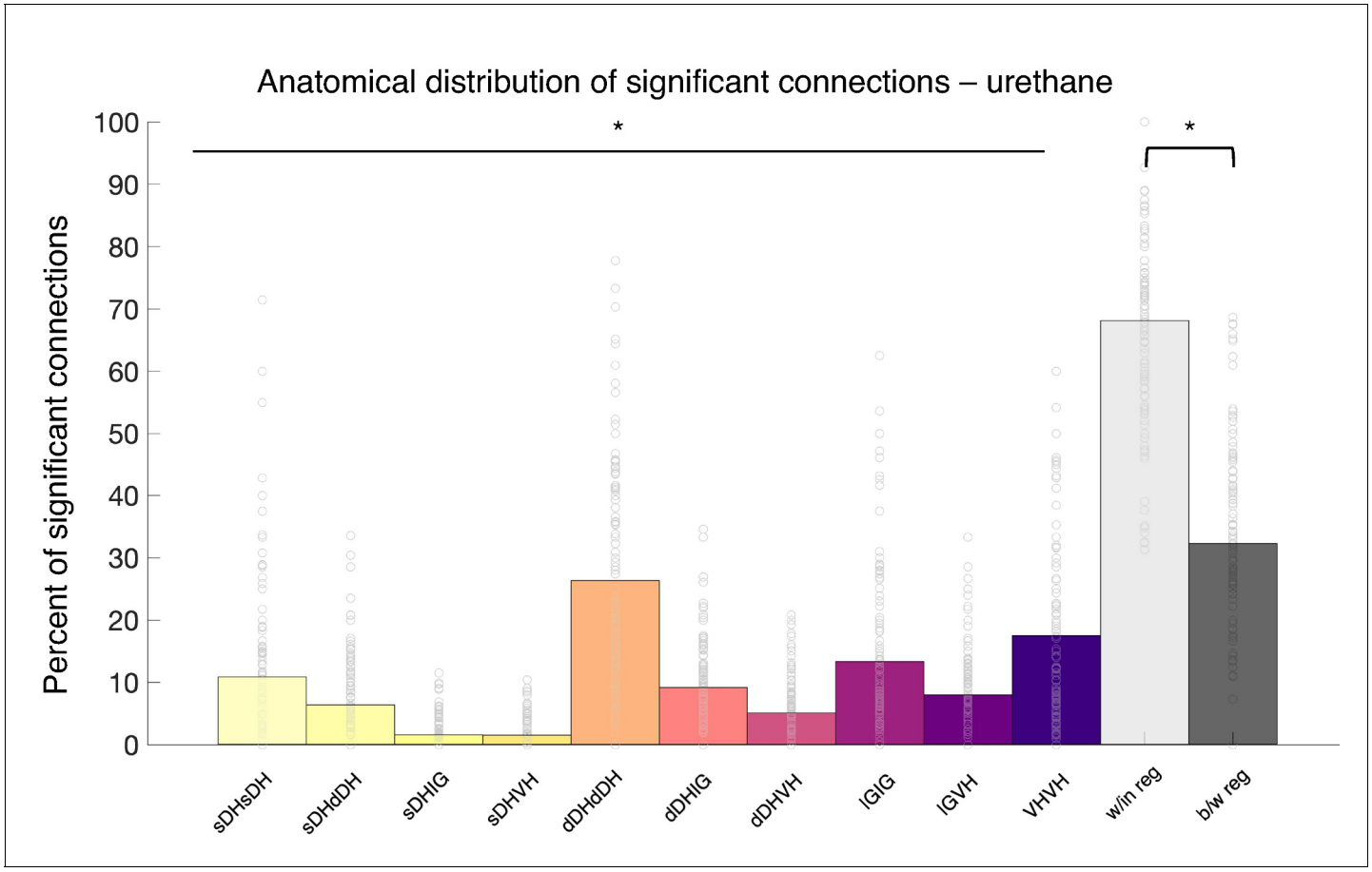

Figure 5—figure supplement 1. Summary of topological data for urethane-anesthetized animals. (**a**) Proportion of significant connections by anatomical region (*N* = 13 animals). From left to right, bar plots indicate connections from sDH-sDH, sDH-dDH, sDH-IG, sDH-VH, dDH-dDH, dDH-IG, dDH-VH, IG-IG, IG-VH, and VH-VH. Darkening color gradient from left to right qualitatively indicates depth from dorsal surface of spinal cord. Grayscale plots are the proportion of within- and between-region connections, respectively. Significant connections are not uniformly distributed anatomically, with an overall main effect of connection location ($p<0.0001$) and significantly more within-region than between-region connections ($p<0.0001$). (**b**) Gross anatomical distribution of the most connected nodes (*N* = 13 animals). From top to bottom (light to dark): sDH, dDH, IG, and VH. Significant main effect of anatomical region on proportion of most connected nodes, $p=0.009$. This figure is analogous to ***Figure 5a*** in the main body; however, here we present raw data (gray circles) superimposed onto the summary bar plots. sDH: superficial dorsal horn; dDH: deep dorsal horn; IG: intermediate gray matter; VH: ventral horn.

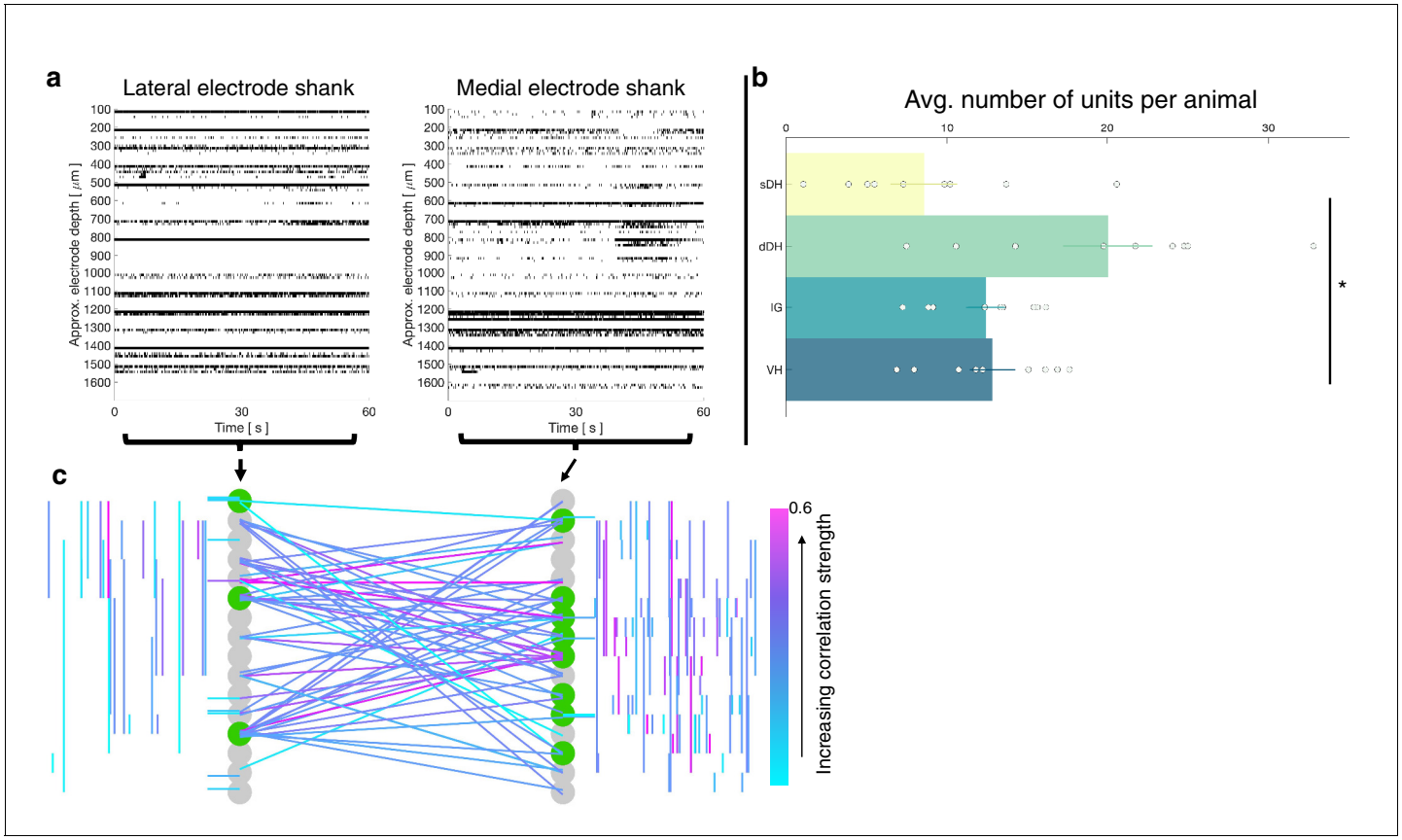

Figure 6. Vigorous spontaneous sensorimotor functional connectivity persists despite preferential depression of ventral horn (VH) cells. (**a**) Raster plot of spontaneously active neurons from a representative isoflurane-anesthetized animal. Each row of hatches represents a discrete neuron. X-axes (time) are synchronized across the two subplots. (**b**) Distribution of spontaneously active units per gross anatomical region across animals in the isoflurane cohort (*N* = 9 animals). The deep dorsal horn contained significantly more spontaneously active units on average than the superficial dorsal horn or VH, driving an overall main effect of region (p=0.001). (**c**) Representative functional connectivity map from panel (**a**). Gray circles represent individual electrodes on the microelectrode array (as in ***Figure 4***). Green highlighted circles were determined to be the most connected nodes of the recording. Colored lines represent significantly correlated temporal discharge between pairs of spontaneously active units at the indicated locations (note: horizontal lines indicate connections between units discriminated from a single electrode, vertical lines are connections between units on the same shank). Line color delineates increasing correlation strength from blue to violet.

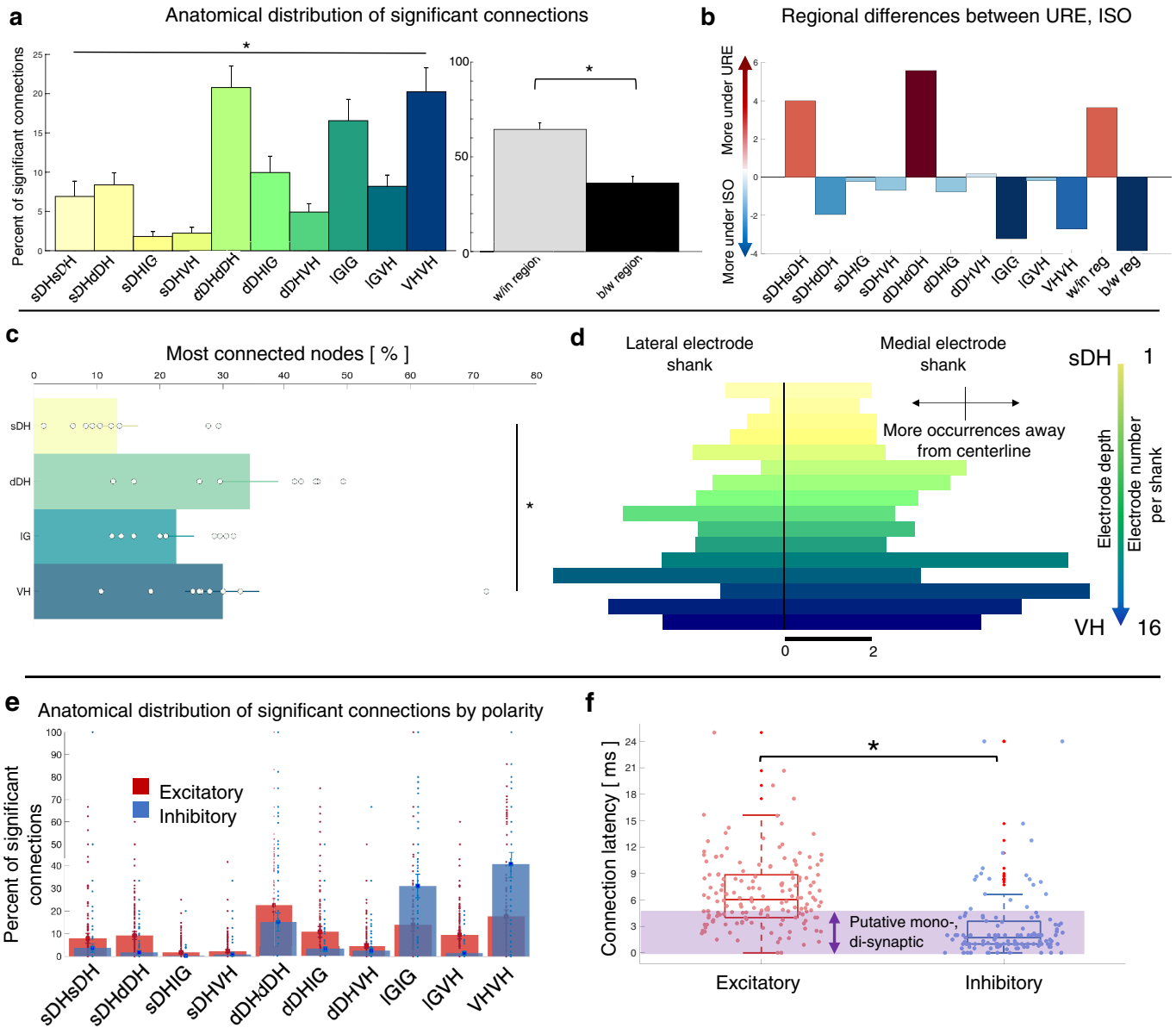

Figure 7. Summary of topological data for isoflurane-anesthetized animals. (**a**) Proportion of significant connections by anatomical region (*N* = 9 animals). From left to right, bar plots indicate connections from sDH-sDH, sDH-dDH, sDH-IG, sDH-VH, dDH-dDH, dDH-IG, dDH-VH, IG-IG, IG-VH, and VH-VH. Darkening color gradient from left to right qualitatively indicates depth from dorsal surface of spinal cord. Grayscale plots are the proportion of within- and between-region connections, respectively. Significant connections are not uniformly distributed anatomically, with an overall main effect of connection location ($p<0.0001$) and significantly more within-region than between-region connections ($p<0.005$). (**b**) Difference in proportion of significant connections per anatomical region between the urethane (URE) and isoflurane (ISO) cohorts. Vertical axis represents the difference in proportion of connections between the two cohorts; positive values: more significant connections in the urethane cohort; negative values: more significant connections in the isoflurane cohort. Overall, there was no statistically significant difference between the anatomical distribution of significant connections between the two cohorts. (**c**) Gross anatomical distribution of the most connected nodes (*N* = 9 animals). From top to bottom (light to dark): sDH, dDH, IG, and VH. Significant main effect of anatomical region on proportion of most connected nodes, $p=0.006$. (**d**) Histogram of most connected nodes across electrodes on each shank. Bars to left of vertical black line reflect lateral electrode shank, and bars to right of vertical black line reflect medial electrode shank; from top to bottom (light to dark), each row represents one electrode (16 total rows). Bar length indicates the number of occurrences that electrode was determined to be in the 'most connected' subset. (**e**) Spatial distribution: proportion of significant connections by polarity (excitatory, inhibitory) and anatomical region in the isoflurane cohort. Red bars: putative excitatory connections; blue bars:

Figure 7 continued on next page

Figure 7 continued

putative inhibitory connections. (**f**) Temporal distribution: latencies of significant excitatory (red) and inhibitory (blue) connections in the isoflurane cohort. Purple shaded region intended to highlight latencies compatible with potential monosynaptic or disynaptic connections. Inhibitory latencies were significantly shorter than excitatory latencies on average within the isoflurane cohort ($p=0.017$). We found no systematic differences in the spatiotemporal profiles of excitatory and inhibitory connections between the urethane and isoflurane cohorts, which preferentially depress the dorsal horns and VH, respectively. sDH: superficial dorsal horn; dDH: deep dorsal horn; IG: intermediate gray matter; VH: ventral horn.

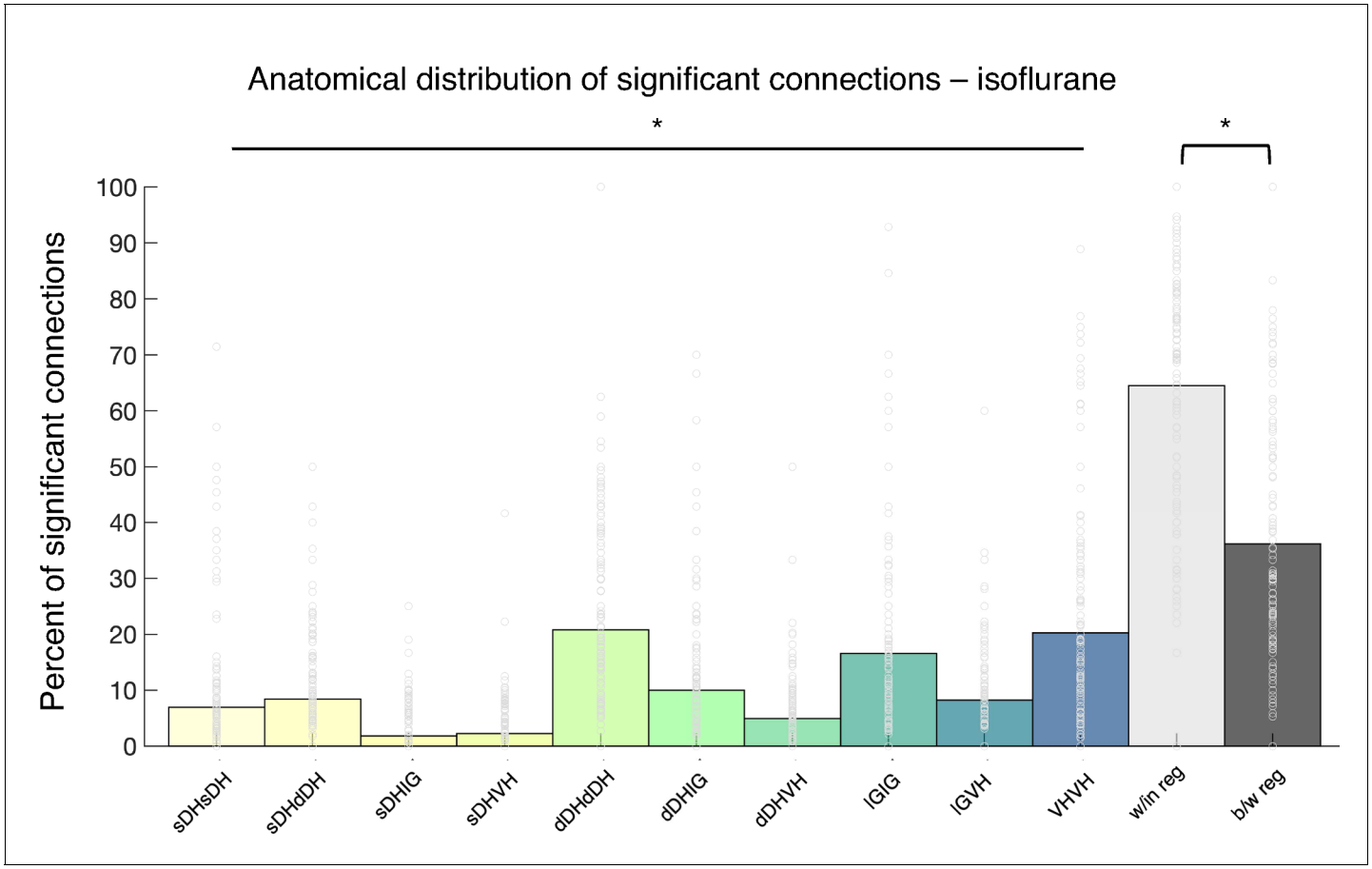

Figure 7—figure supplement 1. Summary of topological data for isoflurane-anesthetized animals. (a) Proportion of significant connections by anatomical region (*N* = 9 animals). From left to right, bar plots indicate connections from sDH-sDH, sDH-dDH, sDH-IG, sDH-VH, dDH-dDH, dDH-IG, dDH-VH, IG-IG, IG-VH, and VH-VH. Darkening color gradient from left to right qualitatively indicates depth from dorsal surface of spinal cord. Grayscale plots are the proportion of within- and between-region connections, respectively. Significant connections are not uniformly distributed anatomically, with an overall main effect of connection location ($p<0.0001$) and significantly more within-region than between-region connections ($p<0.005$). This figure is analogous to ***Figure 7a*** in the main body; however, here we present raw data (gray circles) superimposed onto the summary bar plots. sDH: superficial dorsal horn; dDH: deep dorsal horn; IG: intermediate gray matter; VH: ventral horn.

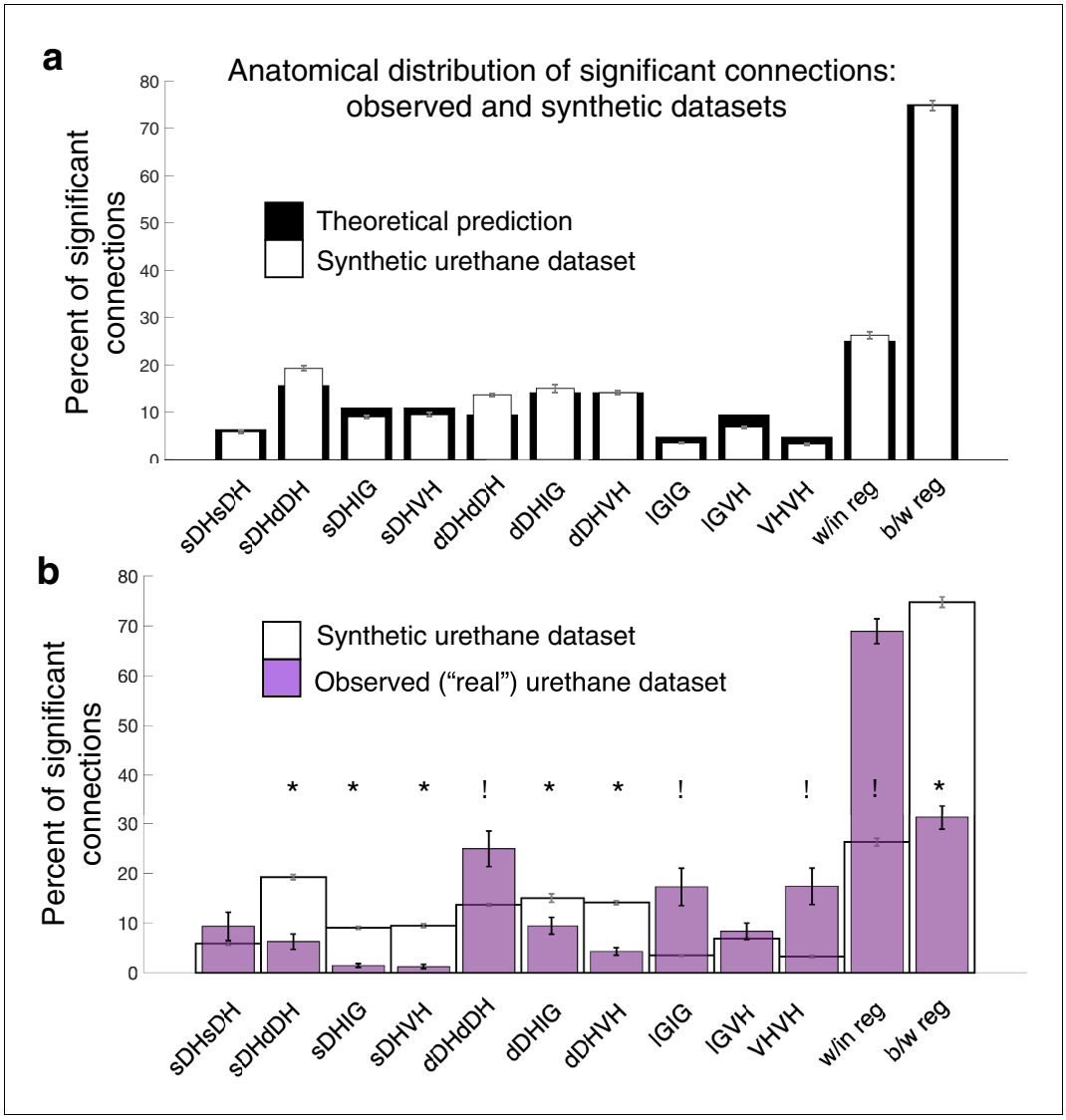

Figure 8. Experimentally realized spatial patterns of functional connectivity diverge from predictions of random network interactions. (**a**) Proportion of significant connections by anatomical region. From left to right, bar plots indicate connections from sDH-sDH, sDH-dDH, sDH-IG, sDH-VH, dDH-dDH, dDH-IG, dDH-VH, IG-IG, IG-VH, and VH-VH. Black bars indicate theoretical predictions; white bars indicate results of simulations ± sem (i.e., synthetic data). The synthetic dataset, generated from randomly shuffling by ±0–5 ms each spike time of each neuron in each trial, then repeating >1000 ×, converges to theoretical predictions. Theoretical predictions are based upon the number and anatomical distribution of electrodes throughout the gray matter. (**b**) Anatomical distribution of synthetic data (white, as in panel **a**) compared to experimentally realized urethane data (*N = 13,* purple bars). We found a significant interaction of cohort by anatomical region (real vs. synthetic, $p<0.0001$), indicating the divergence of the real dataset from that which would be expected by a population of interconnected neurons that are statistically similar but spiking at random. Asterisks indicate connections in which the synthetic data was overrepresented relative to the real data; crosses indicate connections in which the real data was overrepresented relative to the synthetic data. Most notably, we found significantly more within-region connections in the real data compared to the synthetic ($p<0.0001$), and significantly fewer between region connections in the real compared to the synthetic data ($p<0.0001$). sDH: superficial dorsal horn; dDH: deep dorsal horn; IG: intermediate gray matter; VH: ventral horn.

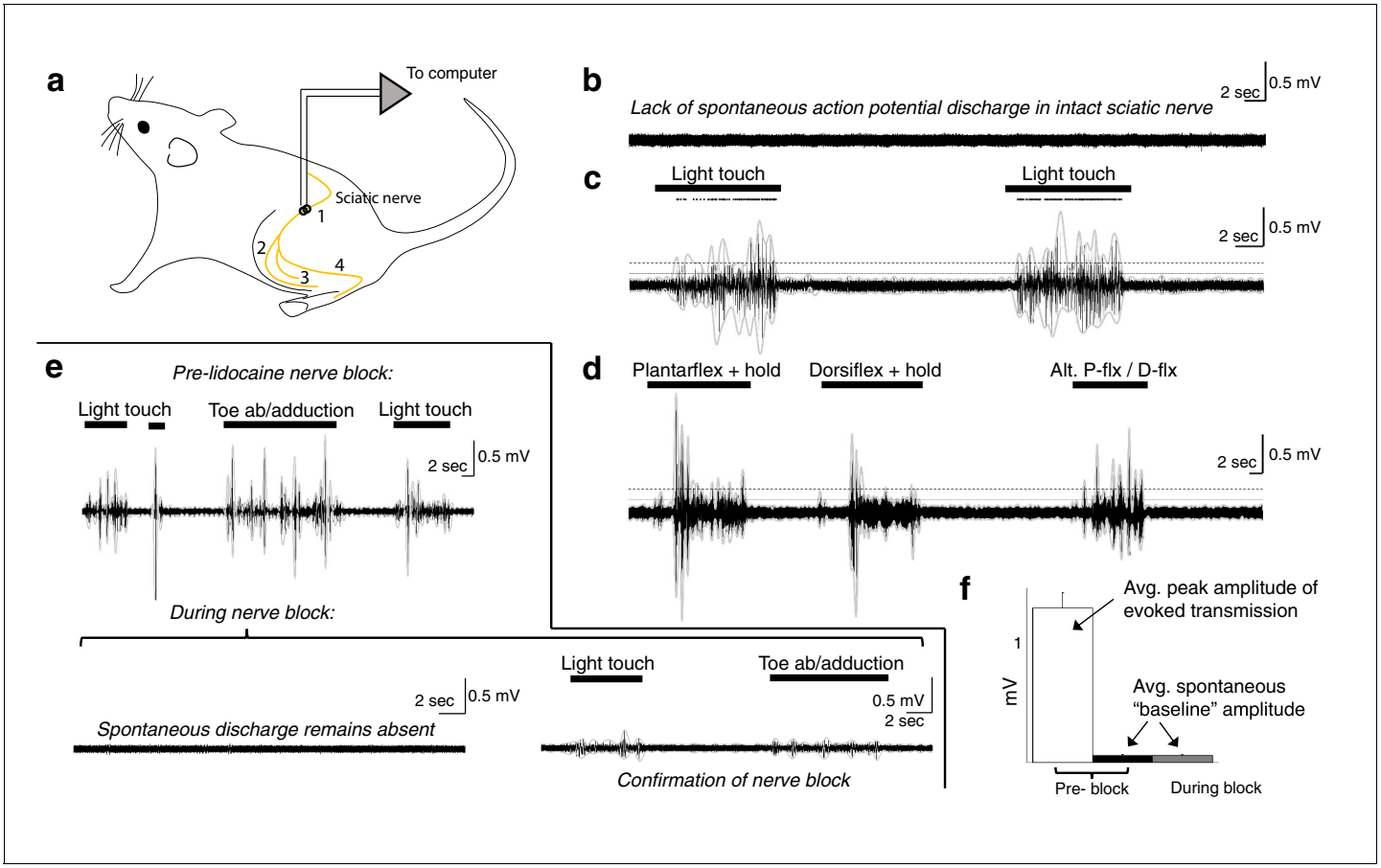

Figure 9. Spontaneous baseline electroneurographic (ENG) activity in the sciatic nerve is minimal and unaltered by nerve block. (**a**) Schematic diagram of recording site and relevant anatomical features. Yellow line indicates the nerve; we recorded sciatic nerve ENG using a hook electrode located at site #1, proximal to the bifurcation into tibial and peroneal nerves; site #2 represents the common peroneal nerve, site #3 represents the sural nerve, and site #4 the tibial nerve. (**b**) Representative ENG activity in the absence of sensory stimulation, as during intraspinal recording sessions. No spontaneous action potential discharge is present, and ENG amplitude is minimal and constant. (**c**) Large bursts of high-amplitude ENG are induced by cutaneous stimulation of the L4–L6 dermatomes. Stimulation epochs are indicated by the top-most horizontal bars, and the dots above the ENG are rasters of individual spikes discriminated from the compound action potential/multi-unit ENG waveforms. The horizontal dashed line indicates the average ENG amplitude during bursts of induced sensory transmission, and the solid horizontal line below it indicates the average ENG amplitude during periods *without* sensory stimulation plus 3× its standard deviation. (**d**) Identical in layout to panel (**c**), with proprioceptive feedback rather than cutaneous. The ankle was plantarflexed and held, dorsiflexed and held, and then alternated between plantarflexion and dorsiflexion. (**e**) Top panel: sciatic nerve ENG recording during periods of induced sensory transmission (horizontal black bars) and baseline transmission prior to lidocaine nerve block. Bottom panel (left): baseline ENG 30 min after epineurial lidocaine injection, showing a lack of spontaneous action potential discharge and minimal amplitude. Bottom panel (right): minimal ENG during attempted induction of sensory transmission confirms efficacy of nerve block. (**f**) Spontaneous baseline ENG amplitude is indistinguishable before (black) and during (gray) nerve block, and is 16.7× smaller than average peak ENG amplitude during bursts of induced sensory transmission before the block (white). Note: the y-axis scales are the same for all plots in (**b–e**).